

Space-time domain velocity distributions in isotropic radiative transfer in two dimensions

Vincent Rossetto

Université Grenoble Alpes / CNRS

Laboratoire de physique et modélisation des milieux condensés

Maison des Magistères - CNRS, BP 166

25, avenue des Martyrs,

38042 Grenoble CEDEX, France

We compute the exact solutions of the radiative transfer equation in two dimensions for isotropic scattering. The intensity and the radiance are given in the space-time domain when the source is punctual and isotropic or unidirectional. These analytical results are compared to Monte-Carlo simulations in four particular situations.

PACS numbers: 42.25.Dd, 05.20.-y

Transport in disordered and random media is a widely addressed physical question which plays an important role in several domains of Physics. Motivated by the kinetic theory of gases, the Boltzmann equation has been studied since more than a century. The radiative transfer equation is a Boltzmann equation where speed is fixed. It was derived by Chandrasekhar [3] to study the radiation transport in a scattering atmosphere. Although radiative transfer is mostly used in three-dimensional systems, the two-dimensional radiative transfer is of interest in several domains, such as seismology, where surface waves carry most of the energy.

Some solutions of the two-dimensional radiative transfer equation are known analytically. For isotropic scattering and isotropic source, the energy distribution has been found by Shang and Gao, and Sato [13, 14] and Paasschens improved these results by providing the radiance distribution [10]. Recent progress in numerical and analytical solutions have been made by Liemert and Kienle [4, 5]. These numerical methods efficiently extend to the three-dimensional case [6, 7]. The situation in two dimensions is more favorable to analytical results for many reasons, geometrical and analytical; let us only mention that the rotation group has a single parameter and that the Green's function has an algebraic Fourier-Laplace transform.

Let us write $q(\mathbf{r}, t, \theta)$ the space-time density of energy flux at position \mathbf{r} at the time t with direction angle θ . $q(\mathbf{r}, t, \cdot)$ is called the *radiance* in the standard terminology in optics. If we integrate the radiance with respect to θ , we get the spatial distribution of energy flux at \mathbf{r} and t . In systems with no absorption, the energy flux distribution integrated over space is constant and normalized to $\frac{c}{\ell}$ in this work.

The differential equation for q is

$$\partial_t q(\mathbf{r}, t, \theta) + c \hat{\mathbf{u}}(\theta) \cdot \nabla q(\mathbf{r}, t, \theta) + \frac{c}{\ell} q(\mathbf{r}, t, \theta) = \frac{c}{\ell} \int_{S^1} \varphi(\theta - \theta') q(\mathbf{r}, t, \theta') d\theta'. \quad (1)$$

The *phase function* φ is an even real valued function describing the distribution of scattering angle. The case

where all scattering angles are equally likely, $\varphi(\theta) = 1/2\pi$, is the *isotropic* case.

To solve the equation (1) we introduce “unscattered” distributions that are the spatial distribution of probability of particles that have not been scattered. These distributions are distinguished by a subscript $_0$. “Scattered” distributions receive the same notations without this subscript. The probability to meet a scatterer on its trajectory at a distance r from the source is $e^{-r/\ell}$, where ℓ is the mean free path. The distribution of particles starting from the origin at time $t = 0$ and moving with speed c with angle θ_0 that have not been scattered at time t is

$$G_0(\mathbf{r}, t, \theta_0) = \frac{c}{\ell} \delta^{(2)}(\mathbf{r} - ct\hat{\mathbf{u}}(\theta_0)) e^{-ct/\ell}. \quad (2)$$

G_0 is the *unscattered energy distribution from an unidirectional point source*. $\delta^{(2)}$ is a two-dimensional Dirac delta function. In the absence of scattering, the propagation angle θ is preserved, its distribution is a Dirac delta-function $\delta(\theta - \theta_0)$. This defines the *unscattered radiance distribution from an unidirectional point source*

$$\mathbb{G}_0(\mathbf{r}, t, \theta; \theta_0) = G_0(\mathbf{r}, t, \theta_0) \delta(\theta - \theta_0). \quad (3)$$

We remark that $\mathbb{G}_0(\mathbf{r}, t, \theta; \theta_0)$ is invariant if one exchanges θ and θ_0 . As a consequence $G_0(\mathbf{r}, t, \theta)$ is also the *unscattered radiance from an isotropic source*. Finally, integrating G_0 over the angle θ , we obtain the *unscattered energy distribution from an isotropic source*

$$g_0(\mathbf{r}, t) = \frac{1}{2\pi} \int_{S^1} G_0(\mathbf{r}, t, \theta) d\theta = \frac{c}{\ell} \frac{\delta(r - ct)}{2\pi r} e^{-ct/\ell}. \quad (4)$$

The distributions defined by Equations (2), (3) and (4) constitute the building blocks for the multiple scattering theory presented in this paper.

Notations and analytic transforms We use the units $c = 1$, $\ell = 1$. We denote by $\tilde{f}(k)$ the spatial Fourier transform of the radial function $f(r)$ and $\hat{f}(s)$ the time Laplace transform of $f(t)$. We will also use the Hankel transform as defined in the appendix A.

The Fourier-Laplace transform of $f(r, t)$ is denoted by $\bar{f}(k, s)$. The leading exponential factor e^{-t} in g_0 ,

G_0 and \mathbb{G}_0 results in the shift of the variable s by 1. All Fourier-Laplace transformed functions carry this shift and are written only with their angular dependences, as in $\overline{G}_0(\theta) \equiv \overline{G}_0(\mathbf{k}, s-1, \theta)$. The Fourier-Laplace transforms of the unscattered distributions admit the following expressions

$$\overline{g}_0 = \frac{1}{\sqrt{k^2 + s^2}}, \quad (5)$$

$$\overline{G}_0(\theta) = (s + i\mathbf{k} \cdot \hat{\mathbf{u}}(\theta))^{-1}, \quad (6)$$

$$\overline{\mathbb{G}}_0(\theta; \theta_0) = \delta(\theta - \theta_0) \overline{G}_0(\theta_0). \quad (7)$$

I. ANALYTICAL DERIVATION

The energy distribution g of the two-dimensional isotropic radiative transfer has been provided by Gao & Shang [14], Sato [13] and Paasschens [10], the latter having also given the radiance solution G . This section is dedicated to the analytical computation of the *scattered radiance from an unidirectional point source* \mathbb{G} . On the way to this result we compute the scattered Green's functions g and G .

A. Solutions in the Fourier-Laplace domain

The radiative transfer equation (1) governing G in the Fourier-Laplace domain rewrites for isotropic scattering

$$(s + i\mathbf{k} \cdot \hat{\mathbf{u}}(\theta)) \overline{G}(\theta) = \tilde{G}(\mathbf{k}, 0, \theta) + \frac{1}{2\pi} \int_{S^1} \overline{G}(\theta') d\theta'. \quad (8)$$

The initial condition $G(\mathbf{r}, 0, \theta) = \delta^{(2)}(\mathbf{r})$ enters into the equation (8) as $\tilde{G}(\mathbf{k}, 0, \theta) = 1$. We multiply the equation (8) by $\overline{G}_0(\theta)$ as given by (6) and we obtain

$$\begin{aligned} \overline{G}(\theta) &= \overline{G}_0(\theta) + \overline{G}_0(\theta) \frac{1}{2\pi} \int_{S^1} \overline{G}(\theta') d\theta' \\ &= \overline{G}_0(\theta) + \overline{G}_0(\theta) \overline{g}. \end{aligned} \quad (9)$$

We notice that \overline{G} will be known as soon as we know \overline{g} . From the integration of equation (9) over θ we get, using the definition (4), the Green-Dyson relation

$$\overline{g} = \overline{g}_0 + \overline{g}_0 \overline{g} \quad (10)$$

and deduce from the expression of \overline{g}_0 in equation (5) the *scattered energy distribution from an isotropic source*

$$\overline{g} = \frac{\overline{g}_0}{1 - \overline{g}_0} = \overline{g}_0 + \overline{g}_0^2 + \overline{g}_0^3 + \dots = \frac{1}{\sqrt{s^2 + k^2} - 1}. \quad (11)$$

Each order of the expansion corresponds to a given number of scattering events the particle has experienced.

From the expression (9) we find the *scattered radiance distribution from an isotropic source* to be

$$\overline{G}(\theta) = \frac{\overline{G}_0(\theta)}{1 - \overline{g}_0} = \overline{G}_0(\theta) + \overline{G}_0(\theta) \overline{g}_0 + \overline{G}_0(\theta) \overline{g}_0^2 + \dots \quad (12)$$

in which we can see that only the last scattering event depends on the angle. Conversely, the *scattered energy distribution from an unidirectional point source* is given by the same formula written as

$$\overline{G}(\theta) = \overline{G}_0(\theta) + \overline{g}_0 \overline{G}_0(\theta) + \overline{g}_0^2 \overline{G}_0(\theta) + \dots$$

in which direction is lost after the first scattering event. If the source is unidirectional, the *scattered radiance distribution from an unidirectional point source* is therefore given by the relation

$$\overline{\mathbb{G}}(\theta; \theta_0) = \overline{\mathbb{G}}_0(\theta; \theta_0) + \overline{G}_0(\theta) \overline{G}(\theta_0). \quad (13)$$

We can now use the solutions (11), (12) and (13) to give the expressions of this functions in the space-time domain.

B. Solutions in the space-time domain

To find the expression of g in the space-time domain we use the simultaneous Hankel-Laplace inverse transform of order zero (see the appendix) with the function $\hat{f}(s) = s/(s-1)$ (and thus $f(t) = \delta(t) + e^t \Theta(t)$) and we obtain

$$g(r, t) = c \frac{e^{-ct/\ell}}{2\pi\ell r} \delta(ct - r) + \frac{e^{-ct/\ell + cT/\ell}}{2\pi\ell^2 T} \Theta(ct - r), \quad (14)$$

the energy distribution from an isotropic source as already found by Shang and Gao and by Sato. We have used the notation $T = \sqrt{t^2 - r^2/c^2}$. Note that the simultaneous inverse transform was performed thanks to the fact that \overline{g} is a function of \overline{g}_0^{-1} . For $t \gg r$, this solution approaches the Gaussian distribution of diffusion, with $D = \frac{1}{2} = c\ell/2$. To compute G we can use the space and time convolution defined by the Equation (9) which yields the expression

$$G(\mathbf{r}, t, \theta) = G_0(\mathbf{r}, t, \theta) + \frac{e^{-ct/\ell}}{2\pi\ell^2} \frac{e^{cT/\ell}}{t - \mathbf{r} \cdot \hat{\mathbf{u}}(\theta)/c} \Theta(ct - r). \quad (15)$$

The expression (15) was first derived by Paasschens [10]. Our work extends his results to the radiance distribution from an unidirectional point source, \mathbb{G} . To compute \mathbb{G} , we use the result (15) together with the relation (13) which defines a convolution in the space-time domain. After integration with respect to the space coordinate we get

$$\mathbb{G}(\mathbf{r}, t, \theta; \theta_0) = \mathbb{G}_0(\mathbf{r}, t, \theta; \theta_0) + \mathbb{G}_1(\mathbf{r}, t, \theta; \theta_0) + \Theta(t - r) \frac{e^{-t}}{2\pi} \int_0^{\frac{t^2 - r^2}{2(t - \mathbf{r} \cdot \hat{\mathbf{u}}(\theta_0))}} \frac{e^{\sqrt{t^2 - r^2 - 2\tau(t - \mathbf{r} \cdot \hat{\mathbf{u}}(\theta_0))}}}{t - \tau - \mathbf{r} \cdot \hat{\mathbf{u}}(\theta) + \tau \hat{\mathbf{u}}(\theta) \cdot \hat{\mathbf{u}}(\theta_0)} d\tau,$$

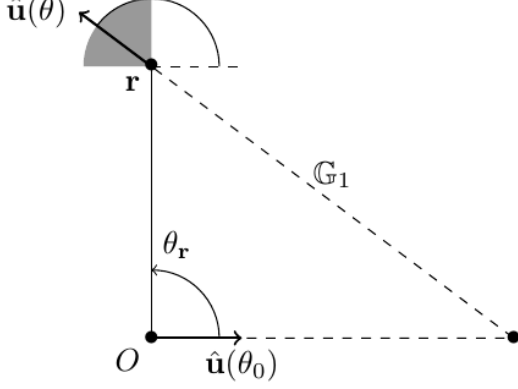


FIG. 1. Description of the geometric variables in the situation where \mathbf{r} and θ_0 are fixed. The trajectory with a single scattering event is drawn as a dashed line. Around the point \mathbf{r} , the shaded region shows the angle interval in which \mathbb{G}_1 contributes to the intensity.

where \mathbb{G}_1 is the single scattering contribution arising from the convolution of G_0 with itself (see the figure 1 and the appendix B).

If $\mathbf{r} = t\hat{\mathbf{u}}(\theta_0)$, the integral vanishes (all the energy is contained in the ballistic term \mathbb{G}_0), otherwise we can perform the change of variable $2(t - \mathbf{r} \cdot \hat{\mathbf{u}}(\theta_0))\tau = t^2 - r^2 - y^2$ and we get for $\theta \neq \theta_0$

$$\mathbb{G} = \mathbb{G}_0 + \mathbb{G}_1 + \frac{e^{-ct/\ell}}{2\pi} \frac{2\Theta(t-r)}{1 - \cos(\theta - \theta_0)} \int_0^T \frac{y e^y}{X^2 + y^2} dy,$$

where X is defined by

$$X = \frac{1}{\ell} \sqrt{\frac{2(ct - \mathbf{r} \cdot \hat{\mathbf{u}}(\theta))(ct - \mathbf{r} \cdot \hat{\mathbf{u}}(\theta_0))}{1 - \cos(\theta - \theta_0)}} - c^2 T^2. \quad (16)$$

We finally obtain our main result for isotropic scattering (with $\theta \neq \theta_0$)

$$\mathbb{G}(\mathbf{r}, t, \theta; \theta_0) = \mathbb{G}_0(\mathbf{r}, t, \theta; \theta_0) + \mathbb{G}_1(\mathbf{r}, t, \theta; \theta_0) + c \frac{e^{-ct/\ell}}{2\pi\ell^3} \frac{2\Theta(ct-r)}{1 - \cos(\theta - \theta_0)} \text{Re} \left[E_1(iX) e^{iX} - E_1\left(iX - \frac{c}{\ell}T\right) e^{iX} \right] \quad (17)$$

The function E_n is the n^{th} order exponential integral function as defined in [1, chap. 5]. The expression (17) has been obtained using the antiderivative 5.1.44 in this reference. In the case where $\theta = \theta_0$, the integral gives the result

$$\mathbb{G}(\mathbf{r}, t, \theta_0; \theta_0) = G_0(\mathbf{r}, t, \theta_0) + \Theta(ct-r) c \frac{e^{-ct/\ell}}{4\pi\ell} \frac{1 + (cT/\ell - 1)e^{cT/\ell}}{(ct - \mathbf{r} \cdot \hat{\mathbf{u}}(\theta_0))^2}. \quad (18)$$

The term G_0 is the unscattered contribution while the second term is a scattered contribution of second order (at least two scattering events have occurred). There are no single scattering contributions from \mathbb{G}_1 in (18).

C. Steady-state solutions

The time-dependent scattered solutions measured at a given point \mathbf{r} exhibit a variety of behaviours that can be exploited when using pulse sources. However, some experimental setups may require the use of a steady source. Hence, we discuss here the steady-state solutions of the radiative transfer equation in two dimensions. We have to first remark that the large time regime is diffusive and as Brownian motion in two dimensions is recurrent, a steady source would yield a diverging energy density as time goes to infinity. However, in the presence of an absorption rate $\mu > 0$, all unscattered and scattered Green's functions get a leading regularizing factor $e^{-\mu t}$. Such a constant rate could come from energy dissipation under another form (like, typically, heat) or account for losses into the third dimension. Since the dimension two is the critical dimension for Brownian recurrence, we expect the

steady-state distribution to diverge logarithmically as μ or r goes to zero.

In the presence of absorption, the steady-state counterpart $f^{\text{ss}}(r)$ of a Green's function $f(r, t)$ is well defined and we have

$$f^{\text{ss}}(r) = \int_0^\infty e^{-\mu t} f(r, t) dt = \hat{f}(r, \mu). \quad (19)$$

It could also be obtained as the inverse Fourier transform of $\tilde{f}^{\text{ss}}(k) = \tilde{f}(k, \mu)$. Denoting by $\alpha = \ell^{-1} + \mu/c$ the total extinction rate, the unscattered energy distribution is $g_0^{\text{ss}}(r) = e^{-\alpha r}/(2\pi\ell r)$ and we show in the appendix C that $g^{\text{ss}} = g_0^{\text{ss}} + g_\infty^{\text{ss}}$ where

$$g_\infty^{\text{ss}}(r) = \frac{1}{2\pi} \sum_{n=0}^\infty \frac{(-\kappa r)^n}{n!} E_{n+1}\left(\frac{\mu r}{2c}\right). \quad (20)$$

with $\kappa = \ell^{-1} + \mu/2c$. The expression (20) is exact and is convenient for small r expansion, where it converges quickly. Using the steepest descent method, we obtain an approximation of $g^{\text{ss}}(r)$ for large r ($r \gg c/\mu$) as

$$g_\infty^{\text{ss}}(r) \underset{r \rightarrow \infty}{\approx} \frac{1}{(2\pi)^{3/2} \ell^2} \frac{e^{-r\sqrt{2\kappa\mu/c}}}{\sqrt{r(2\kappa\mu/c)^{1/2}}}.$$

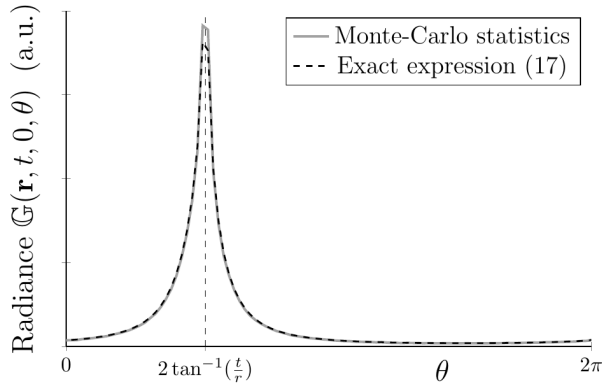


FIG. 2. Radiance for fixed $\theta_0 = 0$, $t = 1.1$ and $\mathbf{r} = (0, 1)$ (thus $\theta_r = \frac{\pi}{2}$) as a function of the propagation angle θ . The Monte-Carlo simulations have been performed until 10^7 trajectories with at least two scattering events are found satisfying the fixed conditions for t and r within $\Delta t = 0.05$ and $\Delta r = 0.05$. A total of 7.16×10^{10} trajectories have been computed.

For large μ ($\mu \gg c/\ell$) we find $g_\infty^{\text{ss}}(r) \approx K_0(\mu r)/(2\pi\ell^2)$. In both cases, we observe a slower energy decay away from the source than for the unscattered energy distribution.

The unscattered radiance distributions are proportional to g_0^{ss} . We easily find $G_0^{\text{ss}}(\mathbf{r}, \theta) = g_0^{\text{ss}}(r)\delta(\theta - \theta_r)$ and $G_0^{\text{ss}}(\mathbf{r}, \theta; \theta_0) = G_0^{\text{ss}}(\mathbf{r}, \theta)\delta(\theta - \theta_0)$. Since the equation (9) states that $\bar{G} = \bar{G}_0 + \bar{G}_0 \bar{g}$ we have $\bar{G}^{\text{ss}} = \bar{G}_0^{\text{ss}} + \bar{G}_0^{\text{ss}} \bar{g}^{\text{ss}}$. The steady-state distributions have the same convolution relations as the time dependent ones. The distribution G^{ss} cannot be computed exactly, but we should remark that near the source, the lowest order of scattering dominates the distribution. The unscattered term, proportional to g_0^{ss} , dominates everywhere it is not equal to zero. A single scattering contribution appears in G^{ss} , we denote it by G_1^{ss} . We can therefore decompose G^{ss} into $G^{\text{ss}} = G_0^{\text{ss}} + G_1^{\text{ss}} + G_\infty^{\text{ss}}$. On the figure 1, the shaded region corresponds to the geometric configuration where the radiance distribution from an unidirectional point source has a contribution from single scattering. If single scattering does not contribute, the main contribution is from double scattering, G_2^{ss} (we do not provide an expression for this contribution). The distribution G^{ss} decomposes into $G_0^{\text{ss}} + G_1^{\text{ss}} + G_2^{\text{ss}} + G_\infty^{\text{ss}}$. The distributions G_1^{ss} and G_∞^{ss} are given in the appendix B.

II. NUMERICAL SIMULATIONS

We compare the solution (17) to statistics obtained from a Monte-Carlo simulation of the two dimensional isotropic Boltzmann equation. We start random walks from the origin at $t = 0$ with propagation angle $\theta_0 = 0$. The step length x is distributed exponentially according to the probability distribution $p(x) = e^{-x}$. After each step, we chose a random angle $0 \leq \theta < 2\pi$ for the propagation.

The figure 1 shows a situation where $\theta_r = \frac{\pi}{2}$ used in the Monte-Carlo simulations. If the random walker

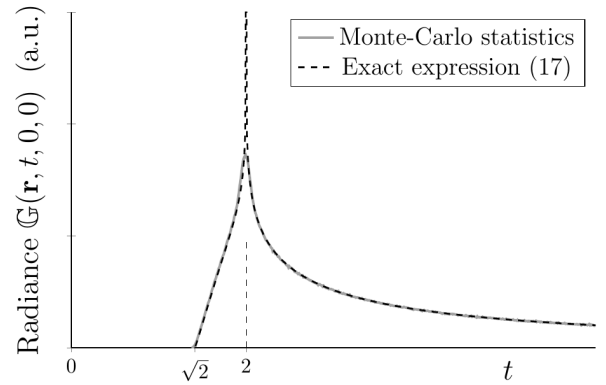


FIG. 3. Radiance in the direction orthogonal to the initial propagation direction as a function of time at the position $\mathbf{r} = (1, 1)$. Single scattering contributions have been removed. The Monte-Carlo simulations have been performed until 10^7 trajectories with at least two scattering events are found satisfying the fixed conditions for \mathbf{r} and θ within $\Delta r = 0.05$ and $\Delta \theta = \frac{\pi}{100}$. A total of 2.85×10^{10} trajectories have been computed.

approaches the “target” position \mathbf{r} by a distance less than Δr between the times $t - \Delta t/2$ and $t + \Delta t/2$, we store the value taken by θ during the corresponding step. The statistics of θ follow the distribution $G(\mathbf{r}, t, \theta, 0)\Delta t \times \pi(\Delta r)^2$. The distribution exhibits a peak at $\theta = 2 \tan^{-1}(\frac{t}{r})$, corresponding to the single scattering trajectory. The results of these simulations is displayed in the figure 2, they compare the distributions of the propagation angle θ for fixed position \mathbf{r} and time t obtained by Monte-Carlo simulations to the predicted formula (17).

The figure 3 displays the radiance at angle $\theta = \pi/2$ as a function of time at the fixed point $\mathbf{r} = (1, 1)$. If the random walker approaches the “target” position \mathbf{r} by a distance less than Δr and the propagation angle θ' is such that $\cos(\theta' - \theta) > \cos(\Delta \theta)$, we store the value of t corresponding to the closest point along the matching step.

The figures 4 and 5 show the radiance at angle $\theta = \theta_0 = 0$, the pathological case where Equation (17) has to be replaced by (B1), as a function of time at the fixed points $\mathbf{r} = (1, 0)$ and $\mathbf{r} = (1, 1)$ respectively. The method is the same as explained for figure 3.

In the figures, the normalization of the numerical distributions has been adjusted, no other parameters have been tuned.

III. OUTLOOK

We have computed the exact solutions of the radiative transfer equation in two dimensions with angular resolution both at the source and the receiver. The time-dependent solutions are useful for the signal analysis when the source is modulated. The steady-state solutions could only be estimated: The approximations we have obtained are asymptotically close to the exact solu-

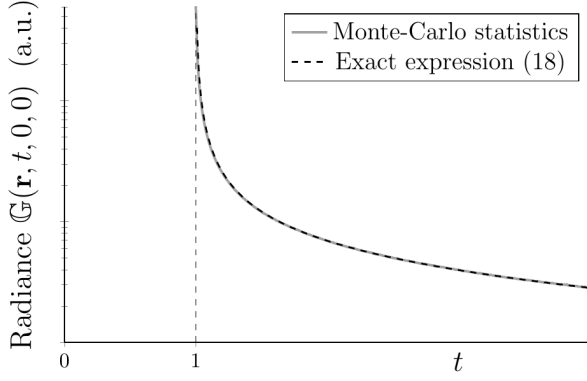


FIG. 4. Radiance in the initial direction of propagation as a function of time at the position $\mathbf{r} = (1, 0)$. Non-scattered contributions have been removed. The Monte-Carlo simulations have been performed until 10^8 trajectories are found satisfying the fixed conditions for \mathbf{r} and θ within $\Delta r = 0.05$ and $\Delta\theta = \frac{\pi}{100}$. A total of 1.49×10^{11} trajectories have been computed.

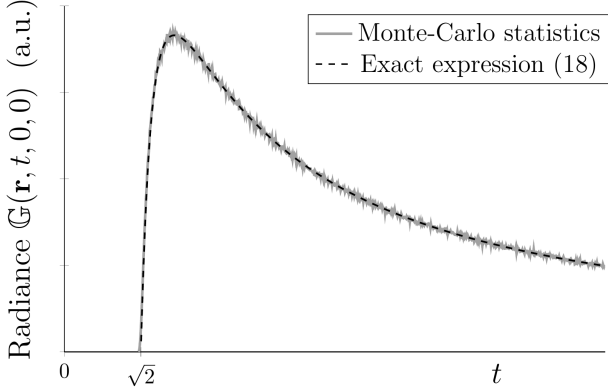


FIG. 5. Radiance in the initial direction of propagation as a function of time at the position $\mathbf{r} = (1, 1)$. Non-scattered contributions have been removed. The Monte-Carlo simulations have been performed until 10^8 trajectories are found satisfying the fixed conditions for \mathbf{r} and θ within $\Delta r = 0.05$ and $\Delta\theta = \frac{\pi}{100}$. A total of 3.77×10^{11} trajectories have been computed.

tions when the absorption is strong or when the distance from the source is large. When absorption is low and the distance from the source is small, the single scattering contribution grows logarithmically and dominates the radiance.

We now briefly discuss the applications of these results. The angular resolution of the theoretical radiance will be useful for analysing data collected with full or partial angular dependences. Angular dependences are easily accessible in optics: Some light sources, such as laser beams, are inherently unidirectional, and collimated receivers can be used to measure the radiance. In acoustics, the so-called beam-forming methods use the signals recorded by an array of aligned receivers to select the sound from an incoming direction. This technique also works with an arrays of sources to produce a unidirec-

tional source of sound. These beam-forming techniques are also frequently used in geophysics as well, with seismic waves. In these fields, using the angular dependences of scattered waves would represent a substantial increase of the available amount of data. We expect that such an increase will help improving imaging methods.

Appendix A: Simultaneous Hankel-Laplace transform

We give here a proof of the simultaneous Hankel-Laplace transformation formula of arbitrary order n . This transformation is more general than the case $n = 0$ used in the main text. The two-dimensional Fourier transform of a function $f(\mathbf{r}) = \sum_{n \in \mathbb{Z}} f_n(r) e^{in\theta_r}$ is by definition $\sum_n i^n e^{in\theta_k} \check{f}_n(k)$, with \check{f}_n the Hankel transform of $|n|^{\text{th}}$ order of f_n .

The n^{th} order Hankel transform of $\delta(r - x)/2\pi r$ is given by $J_n(kx)$. Replacing x by $\sqrt{t^2 - u^2}$ and multiplying by $(t - u)^{n/2}(t + u)^{-n/2}$ we recognize the Laplace transform 29.3.97 in [1] which is equal to $\exp(-u\sqrt{s^2 + k^2}) \xi^n$ with $\xi = k/(s + \sqrt{s^2 + k^2})$. The expression $\exp(-u\sqrt{s^2 + k^2}) \xi^n$ is therefore the n -Hankel-Laplace transform of $(t - u)^{n/2}(t + u)^{-n/2} \delta(r - \sqrt{t^2 - u^2})/2\pi r$. Multiplying both these expressions by an arbitrary function $f(u)$ and integrating from $u = 0$ to infinity we find that

$$\frac{1}{\sqrt{s^2 + k^2}} \left(\frac{k}{s + \sqrt{s^2 + k^2}} \right)^n \hat{f}(\sqrt{s^2 + k^2}) \quad (\text{A1})$$

is the n^{th} order Hankel-Laplace transform of

$$\frac{1}{2\pi} \frac{\Theta(t - r)}{\sqrt{t^2 - r^2}} \left(\frac{r}{t + \sqrt{t^2 - r^2}} \right)^n f(\sqrt{t^2 - r^2}). \quad (\text{A2})$$

We call the transformation between (A1) and (A2) a simultaneous double transform. Simultaneous double transforms have been introduced recently in Ref. [12]. It should be noticed that the simultaneous inversion for anisotropic scattering is possible because the expansion of \mathbb{G} is a rational function of $\bar{g}_0^{-1} = \sqrt{k^2 + s^2}$.

Appendix B: The single scattering functions

The term \mathbb{G}_1 in equation (17) is purely geometric. Its computation is straightforward and yields

$$\begin{aligned} \mathbb{G}_1(\mathbf{r}, t, \theta; \theta_0) &= e^{-ct/\ell} \\ &\delta^{(2)}[(\mathbf{r} - ct\hat{\mathbf{u}}(\theta)) \times (\hat{\mathbf{u}}(\theta_0) - \hat{\mathbf{u}}(\theta))] \\ &\Theta[(\mathbf{r} - ct\hat{\mathbf{u}}(\theta)) \cdot (\hat{\mathbf{u}}(\theta_0) - \hat{\mathbf{u}}(\theta))] \\ &\Theta[ct(1 - \cos(\theta - \theta_0)) - \mathbf{r} \cdot (\hat{\mathbf{u}}(\theta) - \hat{\mathbf{u}}(\theta_0))]. \quad (\text{B1}) \end{aligned}$$

In the steady state regime, it reduces to

$$\mathbb{G}_1^{\text{ss}}(\mathbf{r}, \theta; \theta_0) = \frac{\Theta [\cos(\theta_{\mathbf{r}} - \theta_0) - \cos(\theta_{\mathbf{r}} - \theta) \cos(\theta - \theta_0)]}{4\pi^2 \ell^2 |\sin(\theta - \theta_0)|} \exp \left(-\alpha r \left| \frac{\sin(\theta_{\mathbf{r}} - \theta) - \sin(\theta_{\mathbf{r}} - \theta_0)}{\sin(\theta - \theta_0)} \right| \right). \quad (\text{B2})$$

In the steady-state regime, the contribution of single scattering to the radiance distribution from an isotropic source arises from the convolution of g_0^{ss} and G_0^{ss} , it is equal to

$$G_1^{\text{ss}}(\mathbf{r}, \theta) = \frac{1}{4\pi^2 \ell^2} \exp \left(-\alpha r \cos(\theta_{\mathbf{r}} - \theta) \right) E_1 \left(\alpha r \left(1 - \cos(\theta_{\mathbf{r}} - \theta) \right) \right). \quad (\text{B3})$$

Appendix C: Steady-state approximations

The steady-states solutions and approximations are based on the following expressions. We perform the change of variable $t = \frac{r}{2c} \left(x + \frac{1}{x} \right)$ in the time integral (19) of g given by equation (14) and we get

$$g_{\infty}^{\text{ss}}(r) = \frac{1}{2\pi} \int_1^{\infty} \exp \left(-\frac{\mu r}{2} x - \frac{\kappa r}{x} \right) \frac{dx}{x}.$$

We obtain the equation (20) by expanding the exponential $e^{-\kappa r/x}$ into the series $\sum_n \frac{(-\kappa r/x)^n}{n!}$. The large r approximation is obtained by second order polynomial expansion of $\frac{\mu r}{2} x + \frac{\kappa r}{x}$ around the minimum at $x = \sqrt{2\kappa/\mu}$.

-
- [1] Milton Abramowitz and Irene A. Stegun, *Handbook of mathematical functions*, 10th ed., Dover, 1972.
 - [2] Jérémie Boulanger, Nicolas Le Bihan, and Vincent Rossetto, *Stochastic description of geometric phase for polarized waves in random media*, J. Phys. A: Math. Theor. **46** (2013), 035203.
 - [3] Subrahmanyan Chandrasekhar, *Radiative transfer*, Dover, 1960.
 - [4] André Liemert and Alwin Kienle, *Radiative transfer in two dimensional infinitely extended scattering media*, J. Phys. A : Math. Theor. **44** (2011), 505205.
 - [5] ———, *Green functions for the two dimensional radiative transfer equation in bounded media*, J. Phys. A.: Math. Theor. **45** (2012), 175201.
 - [6] ———, *Light transport in three-dimensional semi-infinite scattering media*, J. Opt. Soc. Am. **29** (2012), 1475.
 - [7] ———, *Explicit solutions of the radiative transport equation in the P3 approximations*, Med. Phys. **41** (2014), 111916.
 - [8] Manabu Machida, George Panasyuk, John Schotland, and Vadim Markel, *The Green's function for the radiative transport equation in the slab geometry*, J. Phys. A.: Math. Theor. **43** (2010), 065402.
 - [9] Nori Nakata, Pierre Boué, Florent Brenguier, Philippe Roux, Valérie Ferrazzini, and Michel Campillo, *Body and surface wave reconstruction from seismic noise correlations between arrays at Piton de la Fournaise volcano*, Geophys Res. Lett. **43** (2016), 1047–1054.
 - [10] J. C. J. Paasschens, *Solution of the time-dependent Boltzmann equation*, Phys. Rev. E **56** (1997), 1135–1141.
 - [11] Vincent Rossetto, *A general framework for multiple scattering of polarized waves including anisotropies and Berry phase*, Phys. Rev. E **80** (2009), 056605.
 - [12] Vincent Rossetto, *Simultaneous double transformations for function depending on space and time*, arXiv:1311.3140, 2013.
 - [13] Haruo Sato, *Energy transport in one- and two-dimensional scattering media: Analytic solutions of the multiple isotropic scattering model*, Geo. Phys. J. Int. **117** (1993), 487–494.
 - [14] T. Shang and L. Gao, *Transportation theory of multiple scattering and its application to seismic coda waves of impulse source*, Scientia Sinica B **31** (1988), 1503–1514.